Low-temperature growth of silicon dioxide films: A study of chemical bonding by ellipsometry and infrared spectroscopy

G. Lucovsky and M. J. Manitini
Department of Physics, North Carolina State University, Raleigh, North Carolina 27695-8202
J. K. Srivastava and E. A. Irene
Department of Chemistry, University of North Carolina, Chapel Hill, North Carolina 27514

(Received 28 July 1986; accepted 16 December 1986)

This paper presents a spectroscopic study using the techniques of ellipsometry and infrared (IR) absorption spectroscopy of the chemical bonding in silicon dioxide (SiO_2) films grown in dry oxygen ambients at temperatures between 550 and 1000 °C. We find that the index of refraction at 632.8 nm increases and the frequency of the dominant IR active bond-stretching vibration at about 1075 cm^{-1} decreases as the growth temperature is decreased below 1000 °C. Comparing the properties of these films with suboxides (SiO_x, $x < 2$) grown by plasma-enhanced chemical vapor deposition, and compacted bulk silica has lead us to conclude: (i) that films grown at temperatures at or below 1000 °C are homogeneous stoichiometric oxides (SiO_2); and (ii) that the systematic and correlated variations in the index of refraction and the IR frequency result from increases in the film density with decreasing growth temperature. We present a microscopic model that accounts for (i) the increases in the density and the index of refraction; and (ii) the accompanying decrease in the IR stretching frequency in terms of a decrease in the Si–O–Si bond angle.

I. INTRODUCTION

The present trend in dielectric thin film research for very large-scale integrated (VLSI) circuit applications is towards thinner films grown or deposited at low temperatures[1]; i.e., below about 900 °C. Silicon dioxide layers for gate insulators in Si device structures are generally grown or annealed at temperatures of at least 1000 °C; however, for many applications it would be desirable to utilize lower oxidation or annealing temperatures (at least below 800 to 900 °C) and at the same time maintain the SiO_2 film and Si/SiO_2 interface quality that are characteristic of oxide layers processed at the higher temperatures. There are numerous studies[2–12] that have shown that both film and interface quality are altered and generally degraded as the oxidation or annealing temperatures are reduced below 1000 °C. In particular, both the oxide fixed charge Q_f and the interfacial trapped charge Q_{it} increase with decreasing processing temperature[2,3] and these increases degrade the performance of oxide/semiductor interfaces in device structures. In addition, the oxide density[4,5] and the intrinsic stress[6,7] have been observed to increase substantially in films grown at temperatures below 1000 °C. It has also been established that the oxidation kinetics change for low-temperature growth, and this has been incorporated into models that have attempted to explain the increase in film stress in terms of the growth process.[8–12] We are currently studying relationships between the electronic and interface properties, the physical properties, and the oxidation kinetics for thin oxide layers grown at different temperatures and/or oxygen pressures. In this paper we will report on one aspect of this study, viz., ellipsometric and IR studies of the chemical bonding in films grown at temperatures between 550 and 1000 °C and over a range of oxygen pressures from 1 to about 300 atm.

Section II presents the experimental aspects of our study; (a) the oxidation procedures and (b) the ellipsometry and IR measurements. Section III discusses the interpretation of the spectroscopic measurements in terms of a model that is based on the local atomic structure. Section IV is a general discussion in which we compare the properties of the low-temperature oxide films with bulk silica. This section of the paper identifies significant differences between films grown below 1000 °C and bulk glasses, wherein the fictive or annealing temperature can be greater than 1000 °C. Finally, Sec. V summarizes the important new results of this study. It also includes our views regarding the significance of our results in the context of a more complete understanding of the differences that can exist in SiO_2 samples that are generated in different ways; e.g., grown oxides versus bulk glasses.

II. EXPERIMENTAL PROCEDURES AND RESULTS

The Si substrates used for the oxide growth were high quality single crystals with a (111) orientation. They were *n*-type (phosphorous doped) with resistivities in the range of 50–100 Ω cm in order to provide transparency in the infrared (IR). The wafers were 0.020-in. thick, had a 1-in. diameter, and were polished on both sides. They were cleaned using the RCA method.[13] This was followed by an HF dip and a thorough rinse in deionized water. The wafers were then blown dry using clean N_2. Oxidation was accomplished using pure dry oxygen at pressures between 100 and 300 atm and at temperatures ranging between 550 to 1000 °C. The high-pressure system used here was a sealed Rene 41 vessel, externally heated by a resistance furnace with pressure and oxygen purity maintained through the use of monel diaphragm compressors. The system is similar to that reported by Zeto *et al.*[14] The vessel contained a fused

 0734-211X/87/020530-08$01.00

silica liner with silica capillaries that were used to decrease the free space in the vessel. At the high oxidation pressures, convection in the vessel can cause temperature changes, thus it is important to minimize the free volume. Because of the residual convection and the fact that the vessel is sealed, the resulting temperature nonuniformities and the possibility of impurities being present combine to reduce the run to run reproducibility with respect to the atmospheric pressure system. Details of the high-pressure system, along with discussions of run to run reproducibility, etc., will be included in a separate publication.[15]

The samples used in both the atmospheric and high-pressure runs were 1-cm-wide strips of silicon cleaved from the 1-in. wafers described above. The oxide thickness was grown to about one-half of an ellipsometric period (approximately 1000 Å) in order to obtain reliable values for the refractive index and the sample thickness from the same measurement. The wavelength for these studies was 632.8 nm and the instrument used was of research quality with polarizer and analyzer angles measured to 0.01°. The optical data were analyzed using a modified version of the program introduced by McCrackin.[16] The uncertainties in the calculated values of n and sample thickness were ± 0.003 and ± 1 A, respectively.

Table I presents the data obtained from the ellipsometry and IR measurements. We have included the growth temperature, the oxygen pressure, the index of refraction n, and the frequency of the dominant IR mode υ in the table. The IR measurements were performed using a Perkin–Elmer Model 983 double beam spectrophotometer. The full width at half-maximum (FWHM) for the dominant IR mode $\Delta\upsilon$ has a value that is essentially the same for all of the oxides we have studied 75 ± 1 cm^{-1}. Under the conditions used for these measurements, the uncertainty in υ is 1 cm and in $\Delta\upsilon$ is 1.5 cm. We have separated the samples into two groups, those grown at an oxygen pressure of 1 atm in part a, and those grown at elevated pressures in part b. Consider first the samples grown at 1 atm of oxygen. We note that as the oxidation temperature decreases, the index of refraction at 632.8 nm increases. These increases in n are accompanied by changes in the IR absorption spectrum. Figure 1 (a) includes a plot of the index of refraction as a function of the oxide growth temperature T_G for the oxide films grown at 1 atm of oxygen. We observe that n decreases as T_G increases and then n tends toward a constant value for temperatures approaching 1000 °C. The ellipsometric data for the films grown at higher pressures do not show close monotonic trends with either oxidation temperature or pressure, as do the oxides grown at 1 atm. This is likely attributed to the experimental complexities associated with high-pressure oxidation vessels as has been mentioned above. However, on the other hand, the high-pressure oxides do display correlations between n and the IR stretching frequency that are essentially the same as those for the films grown at 1 atm of oxygen (see Fig. 3).

Figure 2 gives the IR absorption spectra for three of the films grown at different substrate temperatures and at 1 atm of oxygen. IR spectra for all of the other films we have studied are similar, with the only differences being the position of the strongest absorption peak. The position of this feature varied between about 1060 and 1080 cm^{-1}, and the linewidth, as noted above, remained essentially constant. We have displayed the absorptance A as a function of the wavenumber for the spectral range between 400 and 1500 cm^{-1} in Fig. 2. We have normalized the IR data for reflectance, and then computed A from the transmittance T by the relationship $A = -\ln(T)$. We have examined the absorption over a wider frequency range than is shown in the diagram, viz., from 200 to 4000 cm^{-1}. We were particularly interested in the high-frequency regime, where SiOH and SiH groups can produce absorptions at about 3660 and 2250 cm^{-1}, respectively.[17] We were not able to detect any measurable absorption at these frequencies and, therefore, we conclude that the

TABLE I. Properties of grown oxide layers.

Oxygen pressure (atm)	Oxidation temperature (°C)	Index of refraction (632.8 nm)	IR stretching mode frequency[a] (cm^{-1})
(a) Films grown at 1 atm of oxygen			
1	700	1.486	1066
1	800	1.474	1070
1	850	1.478	1072
1	900	1.466	1076
1	1000	1.465	1077
(b) Films grown at high oxygen pressure			
136	550	...	1066
207	550	1.476	1069
136	600	1.474	1069
212	600	1.484	1068
136	700	1.475	1070
207	700	1.487	1064
212	700	1.476	1074
306	700	1.474	1070
211	800	1.473	1076

[a]The FWHM for the IR stretching mode is essentially the same for all of the grown oxides [parts (a) and (b)], 75 ± 1 cm^{-1}.

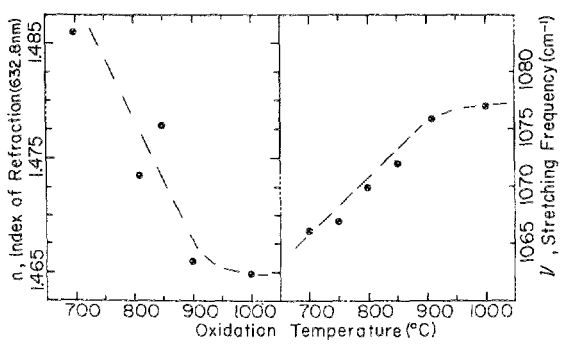

FIG. 1. (a) Index of refraction at 632.8 nm vs oxidation temperature for films grown at 1 atm of dry oxygen. (b) Frequency of IR stretching vibration vs oxidation temperature for films grown at 1 atm of dry oxygen. The dashed lines indicate the trends in the data.

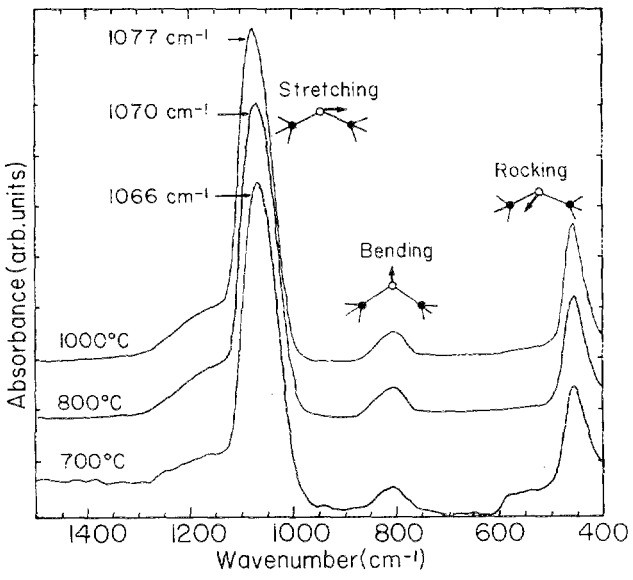

FIG. 2. Normalized IR absorption vs wave number for three films grown at 1 atm of dry oxygen at temperatures of 700, 800, and 1000 °C. The atomic displacements of the three features are also indicated.

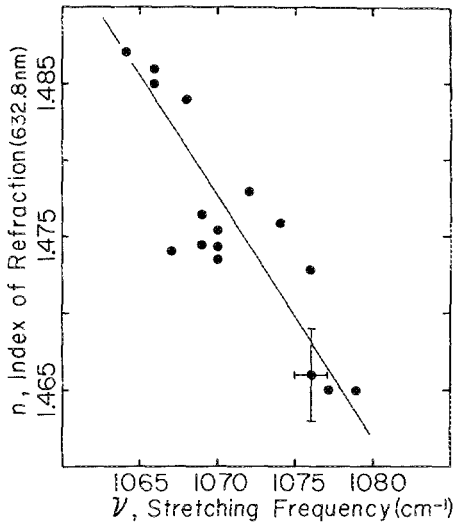

FIG. 3. Index of refraction vs frequency of IR stretching vibration for all low-temperature oxide films. The experimental data are for all of the oxides we have grown and the solid line is derived from our model calculation. We have also indicated the degree of uncertainty by the error bars shown on one of the experimental points.

concentrations of SiH and SiOH groups in our films are less than about 0.5 to 1 at. %, the limit of the IR sensitivity for thin films. The spectra are plotted in the range from 400 to 1500 cm^{-1}, where they display the three characteristic IR bands of the Si–O–Si group.[17,18] The O atom displacements for these vibrations are also indicated in the diagram. In each instance, the Si atom motion is in a direction opposite to that of the oxygen atom.[17,18] The lowest frequency vibration near 450 cm^{-1} is a rocking mode in which the oxygen atom motion is out of the plane of the Si–O–Si bond; the intermediate frequency and weakest absorption at about 800 cm^{-1} is a bending vibration in which the oxygen atom motion is in the plane of the Si–O–Si bond and along the direction of the bisector of the Si–O–Si angle (approximately 150°); and finally, the strongest absorption near 1075 cm^{-1} is a stretching vibration in which the oxygen atom motion is in the plane of the Si–O–Si bond and in a direction parallel to a line joining the two silicon atoms.

Figure 1(b) is a plot of the IR stretching frequency as a function of the growth temperature for the oxides grown at 1 atm of pressure. The IR frequency increases with increasing T_G and tends toward a constant value as T_G approaches 1000 °C. Figure 3 displays the relationship between the stretching frequency v and the index of refraction n; i.e., the IR frequency decreases as the refractive index increases. Figure 3 also includes the IR and ellipsometric data for the films grown at elevated pressures and over a wider temperature range than the data included in Figs. 1(a) and 1(b). We observe the same linear correlation between vibrational frequency and index of refraction in all of the films, those grown at 1 atm of oxygen as well as those grown at elevated pressures, even though n and v for the high-pressure oxides do not display a monotonic scaling with either oxidation temperature (for a fixed pressure) or oxidation pressure (for a fixed growth temperature). The solid line included in Fig. 3 is the result of a model calculation that is presented in the next section.

III. CHEMICAL BONDING IN THE OXIDE FILMS

One of the primary objectives in this study was to be able to interpret the IR and index of refraction measurements in terms of a model based on the local atomic structure of the silicon oxide material in the grown films. We proceed by first considering two possible mechanisms that can account for correlated decreases in the IR frequency and increases in the index of refraction. Mechanism I assumes that as the growth temperature is reduced, the films deviate from SiO_2 stoichiometry with a replacement of Si–O bonds by Si–Si bonds and an accompanying decrease in the molar volume. Mechanism II assumes the composition remains at the stoichiometric point, but the density of the films displays a systematic increase with decreasing growth temperature. Initially, we believed that the first of these two mechanisms might be the only one which could contribute to the decreases we had found in the vibrational frequency for the reasons we discuss below.

Previous studies had shown that the low-temperature films were under compressive stress[4,5] with an accompanying increase in the oxide density.[7,8] We note that the increase in n could be explained by an increase in film density and that a replacement of Si–O by Si–Si bonds could also contribute. We explored the quantitative implications of mechanism I, in particular, we set out to determine if the linear relationship that we had found between n and v (see Fig. 3) was consistent with the behavior expected in suboxide films. Our initial considerations were based on: (i) studies of the IR bond-stretching vibration in suboxide films grown by plasma-enhanced chemical vapor deposition (PECVD)[19];

and (ii) the application of the Lorenz–Lorentz (L–L) (or Clausius–Mossotti) formalism to explain the increases in the index of refraction.[20] For the suboxide films studied in Ref. 19, the shift of the IR stretching frequency was shown to be associated with an inductive effect driven by changes in the local bonding as the oxide composition moved off stoichiometry. In SiO_2, the basic structural unit is the SiO_4 tetrahedron; these are corner connected into a continuous random network structure. Philipp[21] has shown that suboxides formed at low temperatures and not subjected to thermal annealing at temperatures in excess of about 700 °C are single phase and homogeneous with an atomic structure in which there are five different local bonding groups. These are tetrahedra centered about Si atoms with the five possible arrangements of Si and/or O atoms. The systematic decreases in the vibrational frequency, as well as the accompanying increases in the index of refraction, derive from the replacement of Si–O bonds with Si–Si bonds as the composition is changed from SiO_2 to Si. The change in the vibrational frequency is driven jointly by these changes in the local bonding within the tetrahedra (the kinematic effect) and by accompanying decreases in the short range interatom force constants.

The increases in the index of refraction in suboxide films can be understood quantitatively in terms of the (L–L) formalism where two factors contribute: (i) decreases in the molar volume as the Si content is increased; and (ii) differences between the polarizations of Si–O and Si–Si bonds.[20] The L–L relationship is given by

$$\frac{e-1}{e+2}=\frac{4\pi}{3}\frac{N}{V_m}\sum_j (f_j a_j),$$

where $e=n^2$ is the optical frequency dielectric constant, N is Avogadro's number, V_m is the molar volume, and the sum is taken over the polarizabilities a_j of Si–O and Si–Si bonds, and f_j is the fraction of each bond type.

Mechanism I could account for the index of refraction data in a qualitative manner; however, we found several problems with this explanation when we considered the quantitative aspects. First, if we used the IR data to estimate the degree of suboxide character[19] (the value of x for a suboxide designated as SiO_x) and assumed that the molar volume decreased linearly with x, then the calculated values of the index of refraction (L–L model) for the composition characterized by x, were generally higher than those we measured. There was an additional and more serious problem that is illustrated with the help of Fig. 4, where we have plotted the linewidth (FWHM) of the Si–O stretching vibration as a function of the vibrational frequency for both the suboxide films grown by the PECVD method[19] and for the films we have grown. The composition of the suboxide films was determined by electron-beam microprobe analysis.[19] Consider first the PECVD suboxides[19]; the insert in the diagram indicates the line shape of the stretching vibration and the definition of the FWHM. There are two contributions to the FWHM, one from a broadening of the low frequency and dominant component of the line, and the second from the high wave number shoulder that increases in relative amplitude at the same time the low wave number portion of the line broadens. We observe that the FWHM in the PECVD films increases considerably as the oxide composition moves off stoichiometry,[19] but that the FWHM in the low-temperature thermal oxides vary by at most two wave numbers for all of the samples we have so far examined. It is then obvious that the IR feature in the low-temperature oxides is qualitatively different from what has been reported for the PECVD suboxides.[19] The FWHM for thermal oxides does not vary with the vibrational frequency, but rather maintains an essentially constant value over a range of vibrational frequencies in which the FWHM of suboxide films with the same peak value frequencies vary by almost a factor of 20%–30%. We, therefore, observe that the suboxide character is associated with two changes in the IR stretching feature relative to the absorption of stoichiometric SiO_2 (as, e.g., in bulk silica), downward shifts in υ that are accompanied by increases in $\Delta\upsilon$. The comparisons shown in Fig. 4 lead us to conclude that the films we have grown by low-temperature oxidation are not suboxides, but rather are stoichiometric SiO_2, where the shift in stretching frequency derives from a mechanism other than the incorporation of Si–Si bonds.

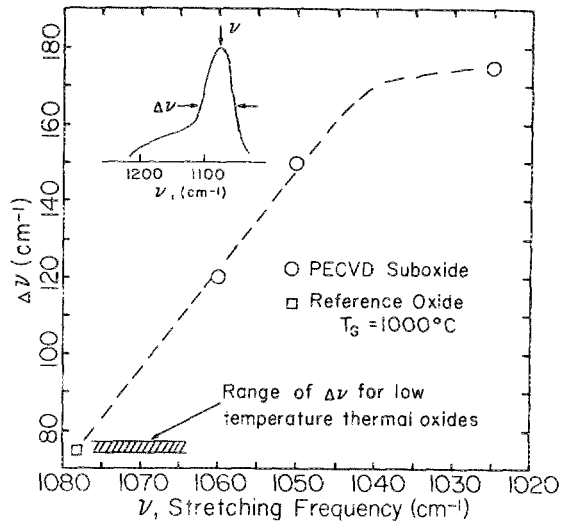

FIG. 4. $\Delta\upsilon$ (FWHM) vs vibrational frequency υ for (a) the low-temperature oxide films we have grown; (b) PECVD oxides (Ref. 19), and (c) a reference oxide grown at 1000 °C. The insert shows a schematic of the line shape defining $\Delta\upsilon$ and υ.

An alternative mechanism that would give rise to systematic increases in n with decreasing growth temperature is mechanism II in which the oxide remains stoichiometric, but becomes compacted and increases in density.[4,5] However, the behavior of the frequency of the stretching vibration would at first sight appear to be at odds with this explanation, simply because we usually expect a bond-stretching frequency to increase with increases in film density in a material that is considered to be three dimensional in its local bonding structure.[22] However, there is ample evidence that this conclusion is not valid for bulk silica, where the frequency of the stretching vibration has in fact been reported to decrease with increased density.[23–25]

Densification of bulk silica is known to occur by several different methods: (i) by the application of high pressures, beyond the elastic limit and generally at temperatures between 400 and 700 °C[26]; (ii) by exposure to intense particle[26] or photon[27] radiation; (iii) by exposure to shock waves[26]; and finally (iv) by heating and quenching in the temperature range between 1000 and 1600 °C.[25] It is, therefore, possible that the decreases in the vibrational frequency in the low-temperature oxides we have grown come from a similar mechanism, namely a relative densification of low-temperature oxide films. This would be consistent with other studies in which the increases in n with decreasing growth temperature have been interpreted in terms of an increasing densification with decreasing growth temperature.[4,5] We can test this explanation by the model calculation that is given below. We would expect that an essentially correct model would yield the linear relationship between n and v that is displayed in Fig. 3.

We consider the local bonding unit of SiO_2 to be the Si–O–Si linkage. In the context of force constant models for the vibrational properties,[18,28] the frequency of the bond-stretching vibration in v-SiO_2 can then be approximated by an expression of the form

$$v^2 = (k/m_0)[\sin^2(\theta/2)] ,$$

where (i) k is a nearest-neighbor effective force constant, which is presumed to vary inversely as the Si–O bond length r_0; (ii) m_0 is the mass of an oxygen atom; and (iii) θ is the Si–O–Si bond angle, assumed to be 144° in v-SiO_2.[23] The expression given above neglects the relative motion of the Si atoms[25]; however, inclusion of the appropriate correction terms to the expression given above does not change any of the qualitative or quantitative aspects of the model, or the conclusions which we will be able to draw. Simon[23] has shown that in radiation compacted material, the Si–O bond length is essentially unchanged, but that the Si–Si distance $d_{Si\text{-}Si}$ is decreased. The Si–Si distance is directly related to the Si–O–Si bond angle by the relationship

$$d_{Si\text{-}Si} = 2r_0 \sin(\theta/2) .$$

This means that changes of v with compaction can be explained in terms of changes in the bond angle at the O atom site. Specifically, as θ is decreased, v also decreases. We can also relate changes in the density to changes in the Si–O–Si bond angle by further assuming that the density of the v-SiO_2 scales inversely as the cube of the Si–Si distance. This relationship has been suggested by several studies on compacted bulk silica.[23,26] We note from the L–L relationship that the index of refraction scales inversely as the molar volume or directly as the density. Combining this assumption relative to the scaling law for the density with the L–L equation and the model for the IR frequency then yields a relationship between the index of refraction and the frequency of the stretching vibration. In particular, v decreases as θ decreases and n increases as θ decreases. If we define an effective dielectric constant e_{eff} by the following expression:

$$e_{eff} = (e-1)/(e+2)$$

then,

$$e_{eff} = (4\pi/3)D'C ,$$

where D' is a normalized density (inversely proportional to $\sin^3\theta/2$) and C is a constant related to the polarizabilities of the constituent Si and O atoms.[20] Since D' is a function of the Si–O–Si bond angle, we can then write that

$$\frac{e_{eff}(1)}{e_{eff}(2)} = \frac{\{\sin^3[\theta(1)/2]\}}{\{\sin^3[\theta(2)/2]\}} = \frac{v(2)^{3/2}}{v(1)^{3/2}} .$$

The straight line relationship between n and v and shown in Fig. 3 is developed from the relationship given above by noting that for an oxide grown at 1000 °C, the vibrational frequency is nominally 1078 cm^{-1} and the index of refraction (632.8 nm) is 1.465. We further assume that the bond angle at the O atom site is 144° for the 1000 °C oxide. We have included in Fig. 3 the values of v and n for all of the samples on which we have performed both ellipsometry and IR studies. We have also indicated the uncertainty in the index of refraction and vibrational frequency measurements. All of the experimentally determined points except one fall within an error bar of the linear relationship predicted by the model. Additionally, we have plotted in Fig. 5 the index of refraction as a function of the relative density, normalized to unity for the film grown at 1000 °C. This in turn suggests that the density increase in the films we have studied can be as large as about 4% as the growth temperature is reduced from 1000 to 700 °C.

IV. COMPARISONS BETWEEN THE PROPERTIES OF DENSIFIED FILMS OF SiO_2 AND BULK SILICA

There have been numerous studies of the densification phenomena in bulk vitreous silica. As noted earlier, densification of bulk v-SiO_2 can be accomplished by the application of pressure beyond the elastic limit, by quenching samples that have been annealed at fictive or soaking temperatures between 1100 and 1600 °C, by exposure to relatively high dosages of particle or photon radiation, or by shock waves. In this section, we discuss the results of these studies as they apply to (i) the degree of compaction relative to the various driving forces, and (ii) the effects of this densification on the optical and vibrational properties, in particular, the index of refraction and the bond-stretching vibrational mode. The

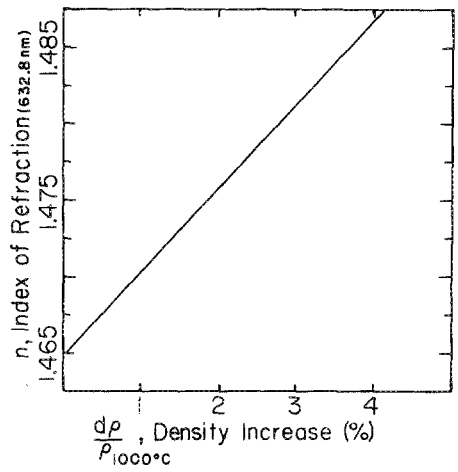

FIG. 5. Calculated variation of n as a function of the relative density.

authors have found that a monograph by Primak is a very useful general reference for this material,[26] and that a handbook of glass data published by Elsevier[29] is an excellent general resource for data, much of it being in graphical form. In discussing compaction in v-SiO_2, we make no attempt to list all available references, but rather highlight the results of those studies which are applicable to our own studies.

Arndt and co-workers[30] have studied pressure induced (permanent) densification in vitreous silica for temperatures below about 700 °C. They found that the degree of densification depends on the applied pressure and the temperature and does not follow any linear scaling laws. At a given temperature, e.g., 500 °C, compaction proceeds most rapidly in the regime above about 6 GPa (about 60 kbar). A pressure of 60 GPa, applied for 10 min at 500 °C results in a densification of approximately 22.6% (the density of the v-SiO_2 increases from 2.2 to 2.7 g/cm^3). At a pressure of about 6 GPa, the densification is temperature dependent with the degree of compaction increasing dramatically for temperatures in excess of about 500 °C. The index of refraction (as measured at the Na D line, 578.0 nm) varies linearly with density increasing from 1.458 in reference samples (quenched from 1000 °C) to 1.47 for a material with a density of approximately 2.565 g/cm^3. (Note that our measurements were made at 632.8 nm.) A number of other studies have shown that the relationship between the index of refraction and density is independent of the way the densification was achieved. These results are summarized in Table II. Simon[23] has shown that the decrease in the frequency of the reflectance peak for the bond-stretching vibration is about 4 cm^{-1} for an applied pressure of 120 000 atm. In addition, Cohen and Roy[31] and Mackenzie[32] have shown that the pressure necessary to achieve a degree of densification between 2.7% and 2.9% varies with temperature and displays a broad minimum (at a level of pressure of about 2 kbar) for temperatures in the vicinity of 1000 to 1200 °C.

Densification by shock waves is qualitatively similar to that induced by static pressure; however, considerably higher pressures can be achieved via the shock-wave approach.[26] The increased pressure range available results in larger degrees of densification with proportionally greater changes in the material properties.[26,29]

Studies of particle induced densification are discussed in the monograph by Primack.[26] The effects of compaction on the index of refraction and the frequency of the IR bond-stretching vibration are qualitatively similar to the effects we have discussed above. For example, an integrated neutron dose of about 2×10^{20} neutrons/cm^2 produces a density increase of about 4% and a decrease in the IR frequency of about 15 cm^{-1}.[23] Radiation compacted material has also been studied by x-ray scattering. For the neutron dose mentioned above, Simon[23] has shown (i) that the nearest-neighbor Si–O distance is unchanged, but (ii) that the Si–Si distance decreases from about 3.03 to 2.99 A. The change in the Si–Si distance is equivalent to a decrease of about 4° in the Si–O–Si bond angle. This in turn has been used by Simon to account for the decrease in the frequency of the IR stretching vibration.[23]

Fiori and Devine[27] have studied radiation induced compaction using ultraviolet radiation with a wavelength of 248 nm. They found that index of refraction was linear in the density and was similar to what occurred for other densification mechanisms; i.e., pressure, neutron bombardment, etc. They further reported that compaction under an integrated dose of 2000 J/cm^3 resulted in a density increase of 16%. This was accompanied by a defect density (detected via spin resonance and consisting primarily of neutral Si dangling bonds, the so-called E' center[33]) of approximately 10^{17}/cm^3.

Densification can also be achieved by thermal annealing in the temperature range between about 1000 and 1600 °C followed by quenching to room temperature.[29] The degree of compaction increases as the annealing or so-called fictive temperature is increased. The degree of compaction has been shown to depend on the OH content of the particular sample of v-SiO_2. The degree of compaction is relatively small; e.g., "low" OH samples (of the order of or less than 0.01% OH) show a density change from 2.201 to 2.203 g/cm^3, whereas "high" OH samples (OH > 0.05%) show about twice the change in density. These changes in density are accompanied by modest changes in the index of refraction; e.g., for low OH silica, the index change is from 1.458 to 1.459 for a change of about 400 °C in fictive temperature.[29] The vibrational properties of v-SiO_2 have been studied by Raman scattering[25] and IR spectroscopy.[24] As the degree of compaction increases, these studies have shown that the frequency of the

TABLE II. Properties of densified silica.

(a)

Sample preparation (densification)	$dn/(dp/p)$ (dimensionless) ± 0.05	$-dv/(dp/p)$ (cm^{-1}) ± 10
(1) Low-temperature thermal oxides (700–1000 °C)	0.55	339
(2) Silica polymorphs	0.55[c]	N.A.
(3) Pressure induced densification	0.45[c]	360[a]
(4) Neutron irradiation (10^{20}/cm^3)	N.A.	360[a]
(5) Thermal annealing (900–1550 °C)	0.51[d]	5280[b]

(b)

Sample	$dn/d(P)$ (1/kbar)
(1) Thermal oxides pressure = film stress	1.1×10^{-2}
(2) Low-pressure studies pressure = 0.0–6 kbar	9.3×10^{-4}
(3) Shock-wave pressure pressure to 500 kbar	4.1×10^{-4}

[a] Reference 21.
[b] Reference 23.
[c] Reference 25.
[d] Reference 27.
[e] Reference 28.

bond-stretching vibration decreases by about 12 cm^{-1} for fictive temperatures between 900 and 1550 °C. We show in Table II that the relationship between n and the density is independent of the way the densification is achieved. However, the variation of the frequency of the IR bond-stretching mode with densification is quantitatively different in the thermally annealed samples than in samples densified at lower temperatures and by the other methods indicated above.

We will now compare our results with those discussed above with the aid of Table II which contains a summary of our data and a compilation of the relevant data for the compacted or densified silica samples. In part (a), we have displayed the various data using derivatives which reflect the changes in both n and the vibrational frequency v relative the fractional changes in the film density (dp/p), and in part (b) we have considered the pressure derivative of the refractive index dn/dP.

Consider first the relationship between the index of refraction and the relative density. This is essentially the same for all of the samples where the relevant data are available. This means that the L–L relationship is obeyed independent of the means by which densification has been achieved. This in turn means that the effective polarizabilities of the O and Si atoms do not depend on the densification mechanism, but only on the resultant density and the atomic packing of the constituent O and Si atoms. On the other hand, the results for the relationship between the frequency of the bond-stretching vibration and the relative density are different.

The densification for the first three samples in part (a) of Table II was achieved at temperatures at or below 800 °C, while the densification in sample 5 was achieved by thermal annealing at temperatures in excess of 900 °C and ranging to 1550 °C. Note that the value of $dv/(dp/p)$ is more than a factor of 10 larger for the thermally annealed densification, while the values of $dv/(dp/p)$ are comparable for our samples and those produced by either pressure or neutron induced densification. We will return to this point in our discussion of the nature of the local atomic structure in densified films. We now consider part (b) of the table. We have previously noted that there is considerable compressive stress in the thermal oxides we have grown and that the amount of stress increases as the growth temperature is reduced.[6,7] The comparisons in part (b) indicate that the relationship between the index of refraction and the film stress is different in our films and those studied either by application of static pressure or by shock-wave pressure. Specifically, the changes we find in the index of refraction with residual stress are more than a factor of 10 higher than those obtained in the other studies. This means that densification in our films is only in part a manifestation of the film stress. Note that the total residual stress in the SiO_2 layer has two components of the same sign (both compressive), one associated with the differences in the thermal expansion coefficients of the SiO_2 film (0.5×10^{-6}/°C) and the Si (5.2×10^{-6}/°C), and the second with an intrinsic film stress that is close to zero for films grown at about 1000 °C and increases to approximately 4 kbar in films grown at 700 °C.[7] The origin of the intrinsic stress is thought to be related to restrictions on the molar volume change between the Si crystal and the SiO_2 layer that is required by the oxidation reaction.[9]

In a parallel way, there appear to be two contributions to the densification, one associated with the total residual stress and the second associated with other aspects of the thin-film growth process. We can demonstrate this by calculating the densification expected on the basis of the stress that is measured in the plane of the oxide film in contact with the Si substrate. If σ is Poisson's ratio, Y is Young's modulus, and P is the total compressive stress, then

$$\Delta V/V = -2(1-2\sigma)(P/Y) .$$

For films grown at 700 °C, P is approximately 6×10^{8} N/m^2. For SiO_2, Y is about 5×10^{10} N/m^2 and σ is about 0.15. This yields a relative decrease in volume with respect to 1000 °C of 1.5%, whereas the refractive index measurements suggest a relative decrease that is at least two times as large (see Fig. 5).

The discussion above and the summary of experimental data displayed in Table II demonstrate that the properties of densified silica can differ depending on the densification mechanism. The most important variable appears to be the temperature range, wherein densification is achieved. We can distinguish two regimes; a low-temperature regime extending to about 1000 °C and a high-temperature regime between about 1000 and 1600 °C. We have shown that in the low-temperature regime that two manifestations of densification, an increase in n and a decrease in the stretching frequency, can be understood in terms of the same atomic model as discussed in the last section. Since the relationship between the vibrational frequency and the density is different in the (high temperature) thermally densified films, this means that a different microscopic model must apply for the determination of the vibrational frequency. Other studies of the elastic properties, in particular of the "rigidity" or shear modulus, have shown that this parameter increases from room temperature to about 900 °C and then drops abruptly in the neighborhood of 1000 °C.[34] The rapid decrease in the shear modulus has been interpreted in a model in which for temperatures above 1000 °C, there is bond rupture and a restructuring of the ring structure of the entire network. This can also be accompanied by changes in the bond angle at the oxygen atom site and by changes in the dihedral angles between Si–O–Si bonding planes. It is clear that additional studies of the short and intermediate range atomic structure by x-ray, x-ray absorbtion fine structure, etc., are necessary before one can resolve this question and understand the differences between the vibrational properties in the two temperature regimes. It is also interesting that a break in the oxidation kinetics, the intrinsic stress, and the interfacial electronic charge (as measured at Si/SiO_2 interfaces) are also observed[35] close to a temperature of 1000 °C.

V. SUMMARY

The results reported in this paper show that when silicon is thermally oxidized below temperatures of 1000 °C, the oxide maintains the SiO_2 stoichiometry, but the molar volume decreases and the density increases. The model that we have

developed to correlate the variation of the IR bond-stretching frequency and index of refraction with temperature indicates that changes in the Si–O–Si bond angle with temperature and, hence, relative densification, are the determining factor in the local atomic structure. However, we find that the degree of densification cannot be accounted for in terms of the total stress that has been measured in the films.[4,5] The conclusion reached previously was that the total stress in the films was in excess of what is generated by the difference between the thermal expansion coefficients of Si and SiO_2 at the growth interface.[7] It was also noted before that the total stress was not adequate to account for changes in the index of refraction with decreasing temperature.[5] Our studies have further substantiated these observations. We have shown that the correlated changes in the refractive index and the stretching frequency could be understood in terms of the same microscopic model of the densification process, namely a decrease in the Si–O–Si bond angle, which in turn promotes a decrease in the Si–Si distance. The model assumes that the density of the film is proportional to the Si–Si distance.

Our discussion has also shown that correlated changes in n and υ are different in bulk silica samples that are thermally compacted by annealing at temperatures in excess of 1000 °C and in thin films grown at temperatures less than 1000 °C. Since the variation of the refractive index with relative density is the same in these high-temperature annealed bulk samples as in the films we have grown, we assume that changes in n can be correlated with changes in the molar volume or density independent of the microscopic nature of the compaction mechanism. This in turn means that changes in the vibrational frequency in the thermally annealed samples, as reported in Refs. 24 and 25, are enhanced by an additional mechanism, i.e., they do not simply scale with the Si–O–Si bond angle as estimated from the densification. This is not surprising when we consider the explanations put forth for the rapid decrease in the value of the shear modulus near 1000 °C. We assume that the ring statistics or intermediate range order are qualitatively different in samples grown or densified below 1000 °C than in samples soaked or annealed at fictive temperatures in excess of 1000 °C. This in turn can account for changes in the short range forces which play an important role in determining the values of the IR vibrational frequencies. This aspect of intermediate range order in thermally grown and vitreous silica needs additional study.

ACKNOWLEDGMENTS

This research has been supported by two ONR contracts, No. N00014-79-C-0133 at NCSU and No. N00014-83-C-0571 at UNC-CH.

[1]E. A. Irene, Semiconduct. Int. **1985**, 92.
[2]B. E. Deal, M. Sklar, A. S. Grove, and E. H. Snow, J. Electrochem. Soc. **114**, 266 (1967).
[3]R. R. Razouk and B. E. Deal, J. Electrochem. Soc. **126**, 1573 (1979).
[4]E. A. Taft, J. Electrochem. Soc. **125**, 698 (1978).
[5]E. A. Irene, D. W. Dong, and R. J. Zeto, J. Electrochem. Soc. **127**, 396 (1980).
[6]E. P. EerNisse, Appl. Phys. Lett. **30**, 290 (1977); **35**, 8 (1978).
[7]E. Kobeda and E. A. Irene, J. Vac. Sci. Technol. B **4**, 722 (1986).
[8]W. A. Tiller, J. Electrochem. Soc. **127**, 619 (1980).
[9]E. A. Irene, B. Tierney, and J. Angillelo, J. Electrochem. Soc. **129**, 2594 (1982).
[10]A. Fargeix, G. Ghibaudo, and G. Kaminarinos, J. Appl. Phys. **54**, 2878 (1983).
[11]R. Doremus, Thin Solid Films **122**, 191 (1984).
[12]J. K. Srivastava and E. A. Irene, J. Electrochem. Soc. **132**, 2815 (1985).
[13]W. Kern and D. A. Poutinen, RCA Rev. **31**, 187 (1970).
[14]R. J. Zeto, C. G. Thornton, E. Hryckowian, and C. D. Bosco, J. Electrochem. Soc. **122**, 1409 (1975).
[15]J. K. Srivastava and E. A. Irene (unpublished).
[16]F. L. McCrackin, Natl. Bur. Stand. Tech. Note 479 (U.S. GPO, Washington, DC, 1969).
[17]F. L. Galeener, Phys. Rev. B **19**, 4292 (1979); F. L. Galeener and P. N. Sen, *ibid.* **17**, 1928 (1978).
[18]P. N. Sen and M. F. Thorpe, Phys. Rev. B **15**, 4030 (1977).
[19]P. G. Pai, S. S. Chao, Y. Takagi, and G. Lucovsky, J. Vac. Sci. Technol. A **4**, 689 (1986).
[20]J. E. Stanworth, *Physical Properties of Glass* (Clarendon, Oxford, 1950), p. 56.
[21]H. R. Philipp, J. Non-Cryst. Solids **8-10**, 627 (1972).
[22]R. Zallen and M. L. Slade, Phys. Rev. B **18**, 5775 (1978); R. Zallen, B. A. Weinstein, and M. L. Slade, J. Phys. Paris **42**, C4 (1981).
[23]I. Simon, in *Modern Aspects of the Vitreous State*, edited by J. D. MacKenzie (Butterworths, London, 1960), p. 120.
[24]P. H. Gaskell and F. J. Grove, in *Proceedings of the 7th International Conference* (International Committee of Glass, Brussels, 1965), Paper 363.
[25]A. E. Geissberger and F. L. Galeener, Phys. Rev. B **28**, 3266 (1983).
[26]W. Primak, *Compacted States of Vitreous Silica* (Gordon and Breach, New York, 1975).
[27]C. Fiori and R. A. B. Devine, in *Defects in Glasses*, edited by F. L. Galeener, D. L. Griscom, and M. J. Weber (Materials Research Society, Pittsburgh, PA, 1986), p. 187.
[28]G. Lucovsky, Philos. Mag. B **39**, 513 (1979).
[29]*Handbook of Glass Data, Part A*, edited by O. V. Mazurin, M. V. Streltsina, and T. P. Shvaiko-Shvaikovskaya (Elsevier, Amsterdam, 1983).
[30]J. Ardnt and D. Stoffer, Phys. Chem. Glass. **10**, 117 (1969); J. Ardnt, *ibid.* **24**, 104 (1983).
[31]H. M. Cohen and R. Roy, J. Am. Ceram. Soc. **44**, 253 (1961).
[32]J. D. MacKenzie, J. Am. Ceram. Soc. **47**, 76 (1964).
[33]C. Fiori and R. A. B. Devine, Phys. Rev. Lett. **52**, 2081 (1984).
[34]R. B. Sosman, *Properties of Silica* (The Chemical Catalogue Co., New York, 1927), p. 447.
[35]E. A. Irene, Philos. Mag. B (to be published).